EFFECTS OF TRANSMISSION LINE READOUT ELECTRONICS ON THE TIMING AND SPATIAL RESOLUTION PROPERTIES OF CHEVRON TYPE MICRO-CHANNEL PLATE PHOTOMULTIPLIER TUBES

Eugene Yurtsev

Office of Science, Science Undergraduate Laboratory Internship (SULI)

University of California

Argonne National Laboratory

Lemont, IL 60439

June 1, 2009

Prepared in partial fulfillment of the requirements of the Office of Science, Department of Energy's Science Undergraduate Laboratory Internship under the direction of Edward May and Karen Byrum at the High Energy Physics Division, Argonne National Laboratory.

Participant: _____

Signature

Research Advisor(s): _____

Signature

TABLE OF CONTENTS

LIST OF FIGURES

ABSTRACT

EFFECTS OF TRANSMISSION LINE READOUT ELECTRONICS ON THE TIMING AND SPATIAL RESOLUTION PROPERTIES OF CHEVRON TYPE MICRO-CHANNEL PLATE PHOTOMULTIPLIER TUBES. EUGENE YURTSEV (University of California, Santa Barbara, CA 93106) EDWARD MAY (High Energy Physics Division, Argonne National Laboratory, Lemont, IL 60439), and KAREN BYRUM (High Energy Physics Division, Argonne National Laboratory, Lemont, IL 60439)

Transmission Line (TL) readout electronics are a natural candidate for the basis of a readout scheme for large area fast photo-detectors built on Micro-Channel Plate (MCP) technology. This paper presents a study of the timing and spatial resolution properties of a 10 micron and a 25 micron Chevron type MCP-PhotoMultiplier Tubes (MCP-PMT) with TL readout. The MCPs were characterized at the Argonne National Laboratory laser test stand facility using a Hamamatsu picosecond laser and a commercial CAMAC system. For each MCP-PMT a timing resolution versus light level scan conducted at two gains near 10^5 in the 15 to 160 photoelectrons range is presented. Both MCPs yielded time resolutions of ~ 10 ps at the 50 photoelectrons level, and demonstrated spatial resolutions $\sim 200\ \mu m$ along the TL at the higher gain and 158 photoelectrons level. These results indicate that the TL readout preserves the intrinsic time characteristics of the MCP-PMT and also provides sub-millimeter spatial resolution along the TL, and thus can serve as the basis for the readout of large area fast photo-detectors. Further studies of TLs implemented on MCP-PMTs of gradually increasing sizes are needed to better understand the issues that may arise while implementing TL readout on large area detectors.

INTRODUCTION

The timing resolution of time-of-flight systems implemented in HEP detectors has not improved significantly in a number of decades, remaining at roughly 100 psecs (pico-seconds) [1]. This limit has been set by the length of the signal amplification path, which is commonly on the order of one inch (100 psecs) in commercial photo-multipliers. The ability to resolve with psec accuracy will, however, vastly expand capabilities in experiments like the LHC, ALICE, Super-B, ATLAS by providing photon vertexing, multiple-interaction separation and charge-particle identification [2].

The Picosecond Timing Project [3] is a collaborative effort to develop large area photo-detectors with picosecond resolution. The proposed detectors will be based on MCP technology in which the amplification path-length is kept small (on the order of a few millimeters), producing output signals that exhibit exceptional time characteristics (e.g., Photek Ltd. reported rise times of $\sim$ 70 ps and FWHM of 110 ps for a 3.2 μm MCP [4]). Such signals enable Time-of-Arrival (ToA) determination with psec precision; in fact, timing resolutions as low as 30 psecs for a single photo-electron have been achieved with MCP Photo-Multiplier Tubes (MCP-PMTs) in the past few years [5, 6].

A significant challenge in constructing such a detector arises in the integration of readout electronics with the MCPs in a way that preserves timing resolution to within a few psecs (i.e., output signals from the MCP anodes are collected over distances that are large in comparison with a psec). Transmission Lines (TLs) have been chosen for the basis of this electronics, and prototype TL readout boards have been designed at the University of Chicago. The boards were mounted on commercially available MCP-PMTs and characterized at the Argonne National Laboratory's test stand. This paper presents the results of these measurements.

MATERIALS AND METHODS

Transmission Line Readout

A 10 μm MCP (XP85022) and a 25 μm MCP (XP85011) were selected for testing the readout boards[1]. These MCPs have 1024 anodes in a square 32x32 arrangement. The TL readout board was constructed to provide 32 50 Ω Transmission Lines and to read out 32 anodes per line. Due to space limitations on the current test board, only 6 of the 32 TLs were made available via SMA connectors. Two SMA connectors (referred to as the top and bottom channels) were connected to the two ends of each available TL. The remaining TLs were terminated in 50 Ω at each end. The TLs are 100 mm in length: 50 mm collect the signals from the anodes and an additional 50 mm carry the signal to the SMA connectors. Printed on an RF ceramic (Rogers 4350B) substrate, the readout board supports bandwidths of up to 3 GHz. Further description of the TL readout board is available in [7]. The board was glued to the anodes using silver conductive epoxy. Figures 1(a) and 1(b) show photographs of the bare TL readout board and of the 25 μm MCP mounted on the TL readout board.

Optics

The MCP-PMTs have been characterized using Argonne National Laboratory's laser test stand. Figure 2 shows the optics arrangement at the laser test stand. A 408 nm laser diode head, driven by a precision laser pulser (Hamamatsu PLP-10 [8]), emits laser pulses at a set rate chosen between a few Hz to a few kHz. The laser light is collimated by a lens to reduce its angular spread, and then attenuated using two neutral density (ND) filters. It passes through a home-made ~ 2000 μm collimator for additional attenuation, and is finally split equally between one photo-detector placed at Leg A and another placed at Leg B. The additional mirrors placed at the light's path at Leg B serve no role except for delaying the light by ~ 5 ns.

[1]Detailed description of the MCPs is available on the manufacturer's website: `http://www.burle.com/`.

Electronics

The test stand uses a commercial CAMAC system to process the output signals from the photo-detectors. Figure 3 shows a schematic of the electronics arrangement used to study the TLs. ORTEC 9327s [9] Constant Fraction Discriminators determine the ToA of photo-detector signals. Then ORTEC 566 [10] Time-to-Amplitude-Converters (TACs) and ORTEC AD114 [11] Analog-to-Digital-Converters (ADC) measure the time difference between selected ToAs. This segment of the electronics enables evaluation of the timing resolution.

LeCroy 2249A ADCs provide pulse height information, enabling determination of the detectors' gains. The ADCs measure the charge in the photo-detectors' signals, offering 0.25 pC resolution with a 5% uniformity over a full scale of 256 pC [12]. ORTEC 9306 1 GHz pre-amplifiers [13] pick up attenuated (by 6 dB) copies of the photo-detector output signals from the discriminators and amplify them (by $\sim$ 34 dB) to the working range of the LeCroy ADCs. In this configuration, the LeCroy ADCs receive photo-detector signals post a 28 dB gain, which means that a photo-detector operating at the single photo-electron level requires a gain of $\sim 10^5$ to produce one ADC count.

The TL-MCP under-study was placed at Leg A. One of its thirty-two TLs was selected and both the top and the bottom channels of the TL[2] were connected to separate ORTEC 9327 discriminators. A 10 um MCP (x85022) based on an 8x8 anode structure was placed at Leg B. Four adjacent anodes were "OR"-ed together and connected to a third CFD, serving as a reference signal for timing measurements. The thresholds of the 9327 discriminators were set to fire on approximately the one photo-electron threshold. Cables from the SMA connectors on the TLs to the 9327 discriminators were kept as short as reasonably possible.

Electronics Noise

Since the MCPs, when operated at high light intensities, were expected to exhibit time resolutions that were similar to the minimum times resolvable using the electronics, it was

[2]The top and bottom channels refer to the two SMA connectors of the TL.

necessary to determine the electronics' contribution to system noise. This was achieved by measuring the time spread of the time difference between two identical signals. The electronics noise was evaluated to be ~ 5 psecs (RMS).

Light Intensity Calibration

The Number of Photo-Electrons (Npe) calibration was carried using a Quantacon PMT [14] operating at a gain of $\sim 10^7$. The light intensity was reduced using the ND filters until the one Npe photopeak appeared. Analysis of the photopeak data in conjunction with the known optical densities of the ND filters[3], allowed to evaluate the average number of photo-electrons at all ND filter configurations.

Measuring Resolutions

The spatial and timing resolutions discussed in this paper are (or are related to) the standard deviations of distributions of the following three time-differences:

$$t_1 = t_{top} - t_{ref}, \tag{1}$$

$$t_2 = t_{bot} - t_{ref}, \tag{2}$$

$$t_{diff} \equiv t_1 - t_2 = t_{top} - t_{bot}. \tag{3}$$

Here, t_{top} and t_{bot} are the ToA of the signals from the top and bottom channels respectively, and t_{ref} is the ToA of the reference signal. t_1 and t_2 are directly measured, while t_{diff} is evaluated by taking the differences between t_1 and t_2 in software.

The signal propagation velocity along the TL can be calculated by measuring the time difference between the signals from the top and bottom channels as a function of position

[3]Calibration data was provided by the manufacturer.

along the TL. This time difference is given by:

$$t(x) = \frac{2x}{v} + c, \tag{4}$$

where x is the position of the incident light on the TL, v is the signal propagation velocity, and c is a constant time delay introduced by the TL and the CAMAC system.

Equation 4 indicates that the spatial resolution along the TL is related to the resolution of t_{diff} as follows:

$$\sigma_x = \sigma_{t_{diff}} \frac{v}{2}. \tag{5}$$

RESULTS

Light Scan

To check the effects of the TL on the timing properties of the MCPs, the time resolutions of the TL MCP-PMTs and of a bare 10 μm MCP-PMT were measured at the same gain (10^5) and different light intensities. The bare MCP-PMT had four anodes "OR"-ed together (like the reference MCP) and was placed at Leg A. Similarly to the TL equipped MCP-PMTs, its timing resolution was determined using the reference signal from the 10 μm MCP-PMT at leg B. The position of the incident laser light remained fixed at the "center" of the detectors during the light scan. Figure 4(a) presents the timing properties of the bare MCP and the two TL MCPs at a gain of $\sim 10^5$. The TL MCP-PMTs have a time resolution similar to the bare MCP-PMT, indicating that no significant signal dispersion or attenuation is caused by the TL. Another comparison between the two TL MCP-PMTs (without the bare MCP) at gain of $\sim 3{\cdot}10^4$ is shown in Figure 4(b). At the lower light intensities, the timing resolution is dominated by photo-statistics, and is expected to scale as $\sim N_{pe}^{-0.5}$ [15]. On the other hand, the timing resolution flattens at the higher light intensities due to the electronics' noise,

which has a larger time jitter than the detector output signals at the higher intensities. The timing resolution is slightly better for the 10 μm MCP than for the 25 μm MCP, which should be expected because the amplification path-length is shorter for the 10 μm MCP.

Position Scan

Figure 5 shows the Timing Resolution vs. Position[4] measured at both the top and bottom channels for 10 μm MCP-PMT TL #5 and the 25 μm MCP-PMT TL #5[5]. The reported timing resolutions (t_1 and t_2) are non-intrinsic, meaning that they include a noise contribution from the electronics and from the reference MCP. Away from the edges, the TL exhibits fairly uniform resolution with a variation smaller than about 2 psecs. There are no significant differences between the two channels, again indicating that the TL introduces minimal attenuation and dispersion. The spike in timing resolution at the center of the 10 um MCP TL #5 likely occurred due to an impedance mismatch (discussed in the following section) between the MCP anodes and the TL board. TL #16 of the 10 μm MCP-PMT was also briefly examined and similar resolutions were obtained (data not shown).

The signal propagation speed along the 10 μm MCP TL #5 was measured to be 105 $\frac{\mu m}{ps}$, exhibiting 1% variations with position and 5% variations between different operating conditions[6]. Simulations of the TL board predicted a velocity of ~ 170 $\frac{\mu m}{ps}$ [7]. The discrepancy between the predicted and measured velocities is likely due to an impedance mismatch. Figure 6 shows the Spatial Resolution vs. Position along 10 μm MCP-PMT TL #5 at three operating conditions. Both the resolution and the resolution uniformity along the TL improve with the Signal to Noise Ratio (SNR)[7]. At 158 photo-electrons and 2.5 kV, the TL delivered spatial resolutions of ~ 200 μm with excellent uniformity across the TL (variations within 20 μm). Again, the worsened resolution at the center of the MCP is likely due to an

[4]Here and in the following figures, the position was adjusted such that the top and bottom channels corresponded to roughly -25 mm and +25 mm respectively, and the center of the TL was at 0 mm.

[5]The #5 refers to the number of the selected TL.

[6]Some of these variations could be an artifact of the measurement system.

[7]The Signal to Noise Ratio is the ratio of the signal's amplitude to the RMS of its baseline.

impedance mismatch, however, as the SNR increases, this effect becomes negligible.

Impedance Mismatch

The existence of an impedance mismatch between the TL readout board and the MCP anodes was verified using Time-Domain-Reflectometry[8]. A fast pulse (with rise time < 90 ps) was fed into one TL channel of a TL-equipped MCP-PMT while the other channel was terminated with 50Ω. The non-terminated channel was monitored with a fast TDS6154C TekTronix scope[9] to check for the existence of reflections. Figure 7 shows the pulse fed into the channel and the subsequent reflection. A similar reflection was seen for the 10 μm MCP-PMT with the TL readout. However, no reflection appeared for a bare TL readout board, indicating that the value of 50 Ω assumed for the impedance of the MCP anodes was somewhat off. Using the formula $\rho = \frac{Z_t - Z_o}{Z_t + Z_o}$ (where ρ is the reflection magnitude, Z_t is the termination impedance and Z_o is the impedance of the transmission medium), the impedance of the transmission medium can be estimated to be 35 Ω. The impedance mismatch, however, is not a serious issue and will be corrected in future designs.

DISCUSSION AND CONCLUSION

The TL equipped MCP-PMTs function as well as the bare MCP-PMT in terms of timing resolution while providing sub-millimeter spatial resolution along the TL. A spatial resolution of ~ 200 μm was demonstrated here, however, better resolutions are attainable at higher gains and/or light levels. Simulations results in [17] indicate that waveform sampling will outperform the constant fraction discrimination technique, so Application Specific Integrated Circuits dedicated for waveform sampling will further improve the timing and spatial resolutions. The TL readout also offer spatial resolution in the transverse dimension. This resolution depends on the "density" of the TLs in transverse dimension, and can be

[8]For more information, see, for example, reference [16].

[9]Spec sheet available at `http://www.tequipment.net/TektronixTDS6154C.html`

determined through measurement of the relative pulse heights of adjacent TLs. The TL readout reduces the number of readout channels (e.g., the 1024 MCP anodes turn to just 64 channels), and allows this number to scale with a single detector dimension (either its length or width), rather than with the area. This feature will offer significant reduction in system costs for large detectors. The TL readout scheme works well with the MCP-PMTs tested, and is ready to be prototyped in larger systems to begin addressing any scale-up related challenges that may arise.

ACKNOWLEDGMENTS

This work was supported by the High Energy Physics division at Argonne National Laboratory, the Department of Energy and the Office of Science. The ROOT analysis package was used for data analysis, GNUplot to create the plots, and Inkscape to draw the optics and electronics diagrams. I would like to thank my advisors Edward May and Karen Byrum. I would also like to thank Jean-Francois Genat for providing the TL readout board photographs, and my office-mate, Tyler Nussbaum, for providing me with a lively working environment.

REFERENCES

[1] W. Klempt, "Review of particle identification by time of flight techniques," *Nuclear Instruments and Methods in Physics Research A*, vol. 433, pp. 542–553, aug 1999.

[2] Henry Frisch, et al., "The Development of Large-Area Fast Photo-detectors," Will be available on pico-second main webpage., May 2009, proposal Submitted to DOE. [Online]. Available: http://psec.uchicago.edu/

[3] Main webpage of the Picosecond Timing Project. [Online]. Available: http://psec.uchicago.edu/

[4] J. Milnes and J. Howorth, "Advances in Time Response Characteristics of Micro-Channel Plate PMT Detectors," Available on Photek website., Photek Ltd, 26 Castleham Road, St Leonards on Sea, East Sussex TN38 9NS US. [Online]. Available: http://photek.com/support/Papers/Advances%20in%20Time%20Response%20Characteristics%20of%20Micro-channel%20Plate%20PMT%20Detectors.pdf

[5] J. Va'vra, J. Benitez, D. W. G. S. leith, G. Mazaheri, B. Ratcliff, and J. Schwiening, "A 30 ps timing resolution for single photons with multi-pixel burle mcp-pmt," *Nuclear Instruments and Methods in Physics Research A*, vol. 572, no. 1, pp. 459–462, 2007.

[6] M. Akatsu, Y. Enari, K. Hayasaka, T. Hokuue, T. Iijima, K. Inami, K. Itoh, Y. Kawakami, N. Kishimoto, T. Kubota, M. Kojima, Y. Kozakai, Y. Kuriyama, T. Matsuishi, Y. Miyabayashi, T. Ohshima, N. Sato, K. Senyo, A. Sugi, S. Tokuda, M. Tomita, H. Yanase, and S. Yoshino, "MCP-PMT timing property for single photons," *Nuclear Instruments and Methods in Physics Research A*, vol. 528, no. 3, pp. 763–775, August 2004.

[7] F. Tang, K. Byrum, H. J. Frisch, J.-F. C. Genat, M. Heintz, E. N. May, T. Natoli, and E. Yurtsev, "Position Sensing using Pico-Second Timing with Micro-Channel Plate Devices and Waveform Sampling," April 2009, preprint submitted to Elsevier Science.

[8] "Hamamatsu Picosecond Pulser PLP-10," Hamamatsu Website. [Online]. Available: http://sales.hamamatsu.com/assets/pdf/hpspdf/PLP-10.pdf

[9] "9327 1-GHz Amplifier and Timing Discriminator," ORTEC Website, 2007. [Online]. Available: http://www.ortec-online.com/electronics/amp/9327.htm

[10] "566 Time-to-Amplitude Converter," ORTEC Website, 2007. [Online]. Available: http://www.ortec-online.com/electronics/tac/566.htm

[11] "AD114 CAMAC 16k ADC," ORTEC Website, 2007. [Online]. Available: http://www.ortec-online.com/electronics/adc/ad114.htm

[12] "2249A CHARGE ANALOG-TO-DIGITAL CONVERTER," LeCroy Website, 1995. [Online]. Available: http://www.lecroy.com/lrs/dsheets/2249.htm

[13] "9306 1-GHz Preamplifier," ORTEC Website, 2007. [Online]. Available: http://www.ortec-online.com/electronics/preamp/9306.htm

[14] "8850 Photomultiplier," Burle Website. [Online]. Available: www.burle.com/cgi-bin/byteserver.pl/pdf/8850.pdf

[15] Hamamatsu, *Photomultiplier Tubes: Basics and Applications*, 3rd ed., Hamamatsu, 2006. [Online]. Available: http://sales.hamamatsu.com/assets/applications/ETD/pmt_handbook/pmt_handbook_complete.pdf

[16] D. J. Dasher, "Measuring Parasitic Capacitance and Inductance Using TDR," *Hewlett-Packard Journal*, p. 8, April 1996.

[17] J.-F. Genat, G. Varner, F. Tang, and H. Frisch, "Signal Processing for Pico-second Resolution Timing Measurements," 2008. [Online]. Available: http://www.citebase.org/abstract?id=oai:arXiv.org:0810.5590

FIGURES

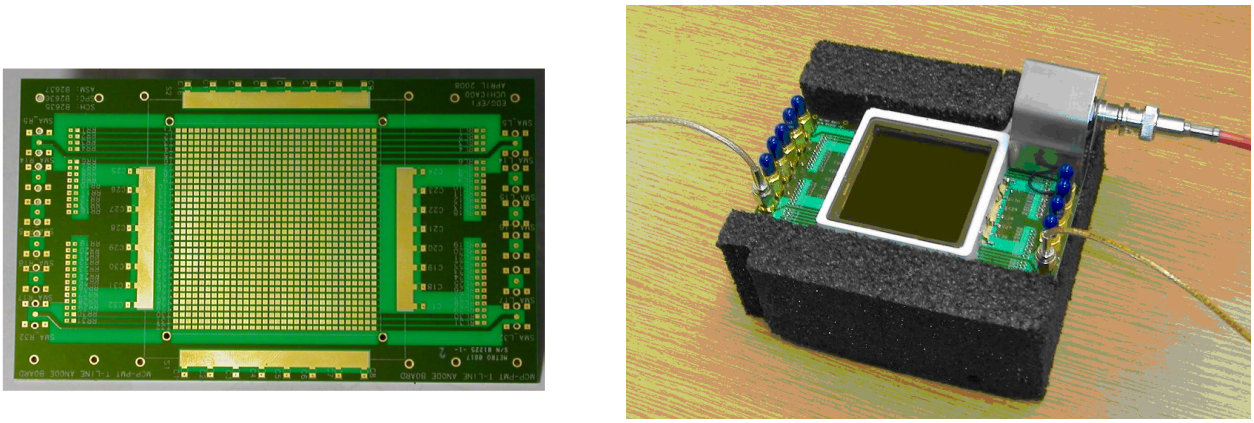

(a) Bare TL board.

(b) 25 μm MCP-PMT mounted on the board.

Figure 1: (a) The bare TL readout board. The TLs are 100 mm in length: 50 mm to collect the signals from the anodes and 50 mm to carry it to the SMA connectors. (b) 25 μm MCP-PMT mounted on the readout board. The board was glued to the MCP anodes using silver conductive epoxy in such a way that each TL covered a row of 32 anodes.

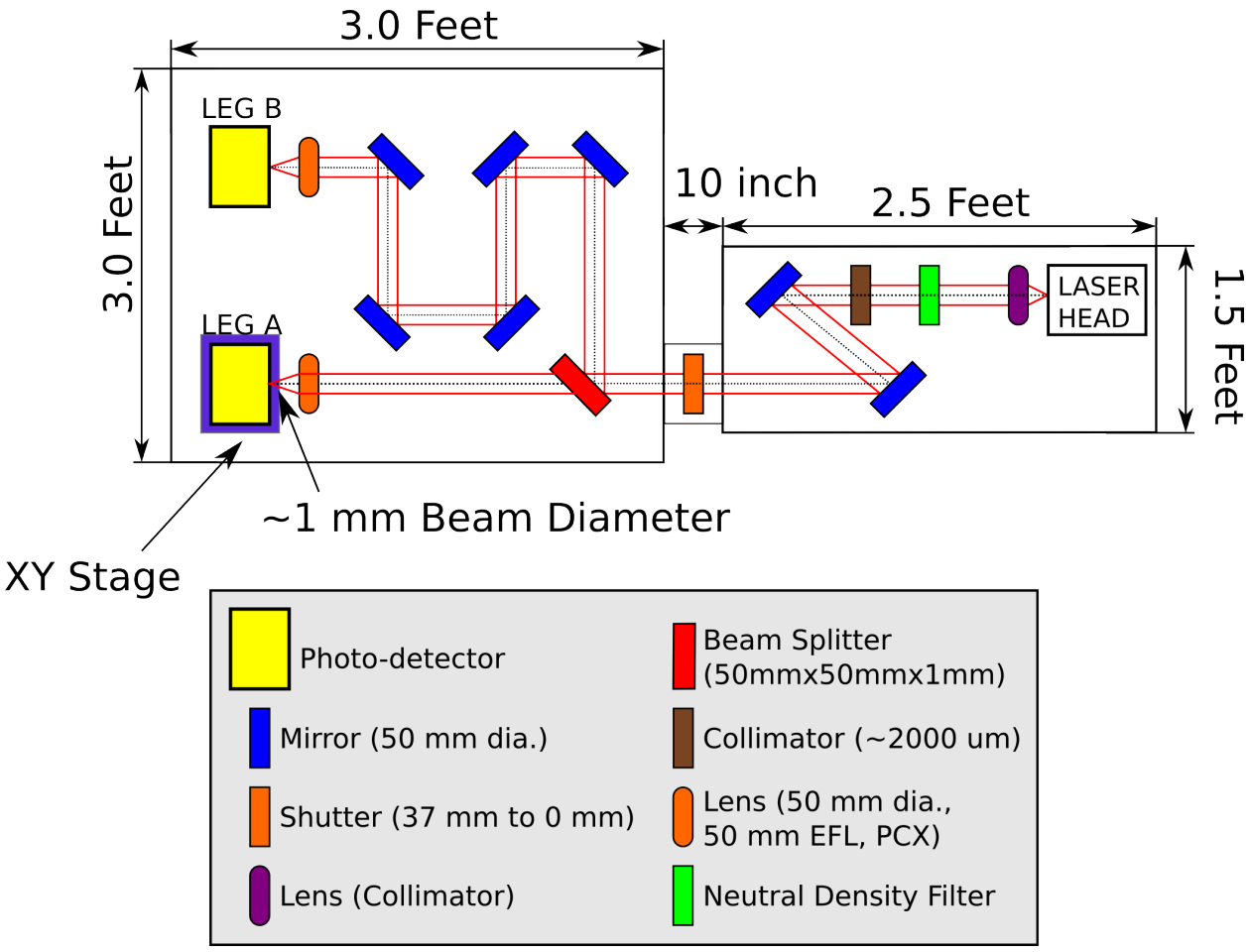

Figure 2: The laser diode head emits 408 nm light. This light is collimated by a laser lens, and then attenuated using two neutral density filters. It passes through a home-made $\sim$ 2000 μm collimator for additional attenuation, and is finally split equally between one photo-detector placed at Leg A and another placed at Leg B. The additional mirrors placed at the light's path at Leg B serve no role except for delaying the light by $\sim$ 5 ns. The light is focused to a $\sim$ 1 mm diameter spot on the detectors. The XY stage at Leg A allows to scan across the detector and characterize the dependence of the timing and spatial resolutions on the spatial position.

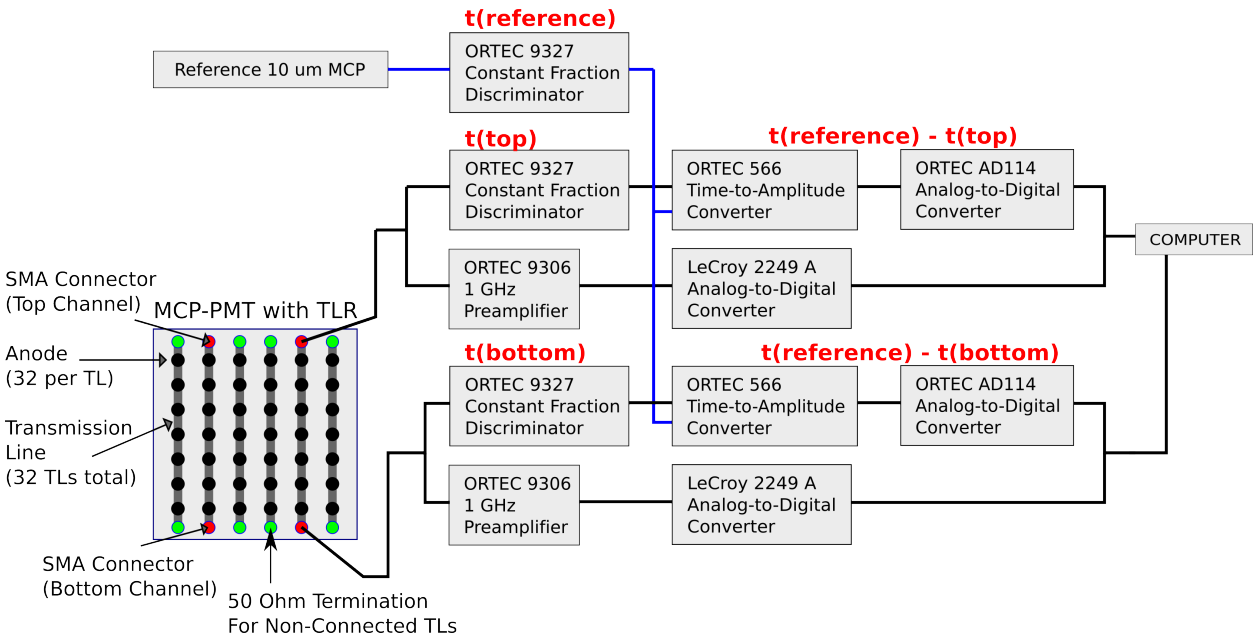

Figure 3: A schematic of the electronics system used at the laser test stand. Time-of-Arrival is obtained using the constant fraction discrimination technique. ORTEC 566s determine the time difference between a TL channel and the reference signal. ORTEC 9306s pick up attenuated (by 6 dB) versions of the output signals from the discriminators and amplify them (by $\sim$ 34 dB) to the working range of the LeCroy ADCs. The noise contribution of the electronics at high light intensities was evaluated to be $\sim$ 5 ps.

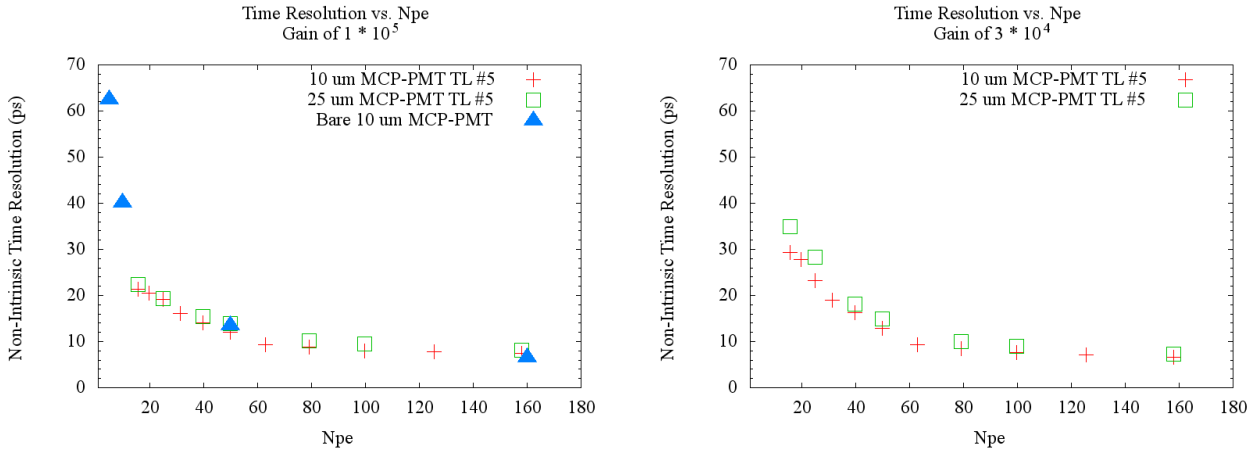

(a) Time resolutions at a gain of $1 \cdot 10^5$.

(b) Time resolutions at a gain of $3 \cdot 10^4$.

Figure 4: (a) A comparison between the time resolution of a bare 10 μm MCP-PMT and the 10 μm and 25 μm MCP-PMTs with the TL readout board at a gain of $1 \cdot 10^5$. The TL does not introduce any significant deterioration to the resolution. (b) Comparison between the two MCP-PMTs with the TL readout board at a gain of $3 \cdot 10^4$. The timing resolution is limited by the electronics noise ($\sim$ 5 ps), which is responsible for the flattening shape of the resolution at higher light intensities.

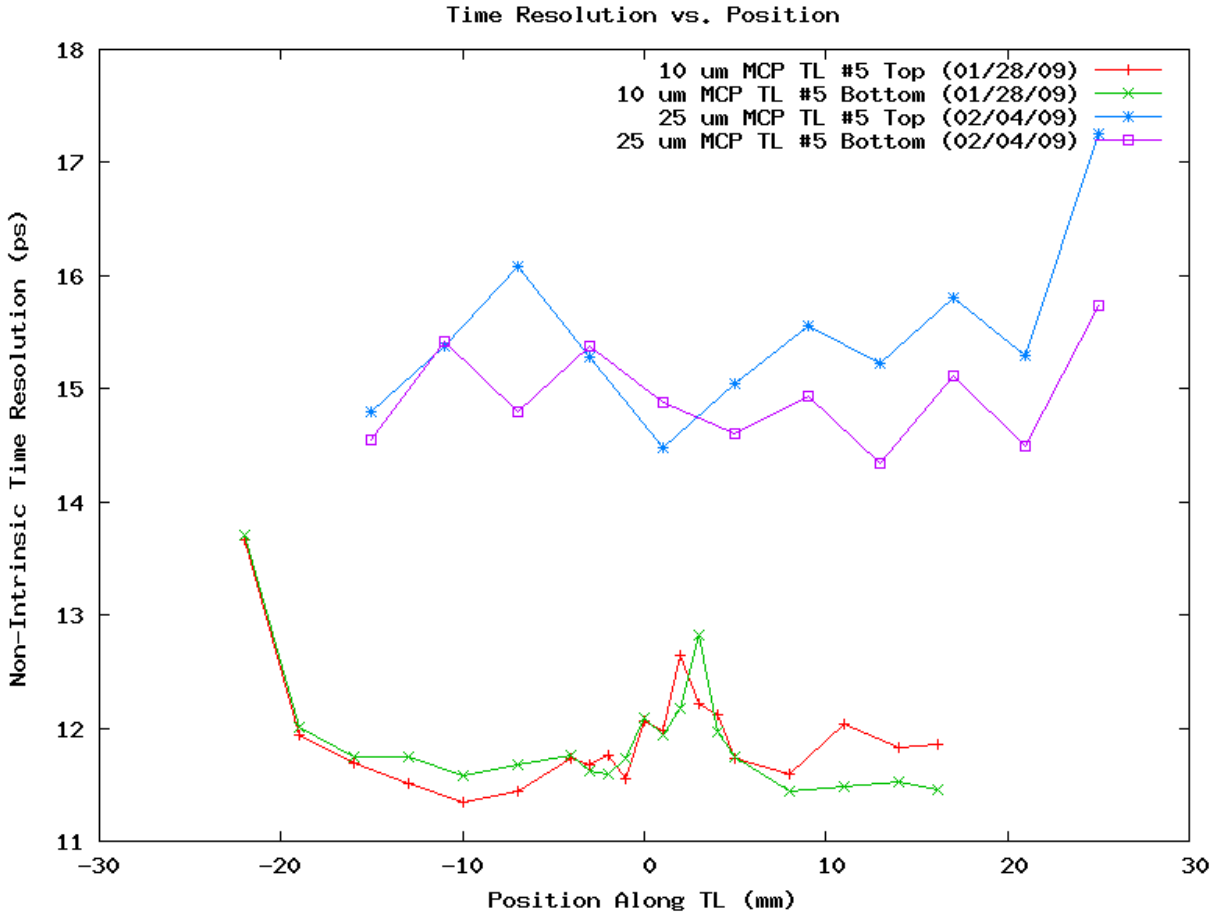

Figure 5: Time Resolution vs. Position along the TL monitored at both TL channels. The resolution remains nearly uniform within away from the edges. The timing resolution as measured by the top and bottom channels agree with one another, indicating that the TL introduces only minimal dispersion and attenuation.

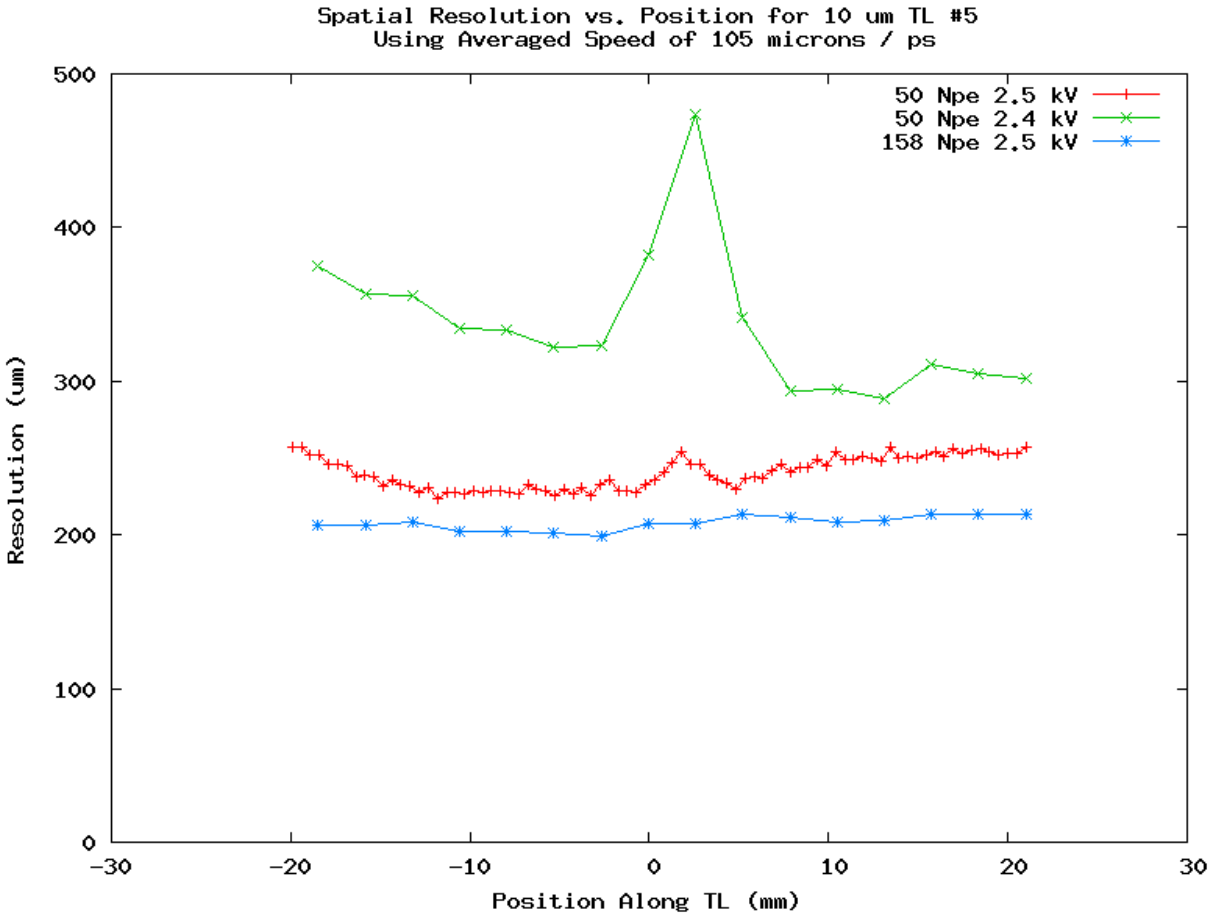

Figure 6: Spatial resolution along 10 μm MCP-PMT TL #5 under three conditions. At the 158 Npe level and a voltage of 2.5 kV, the TL demonstrates a spatial resolution of nearly 200 μm. Both resolution and resolution uniformity improve with higher signal to noise ratios.

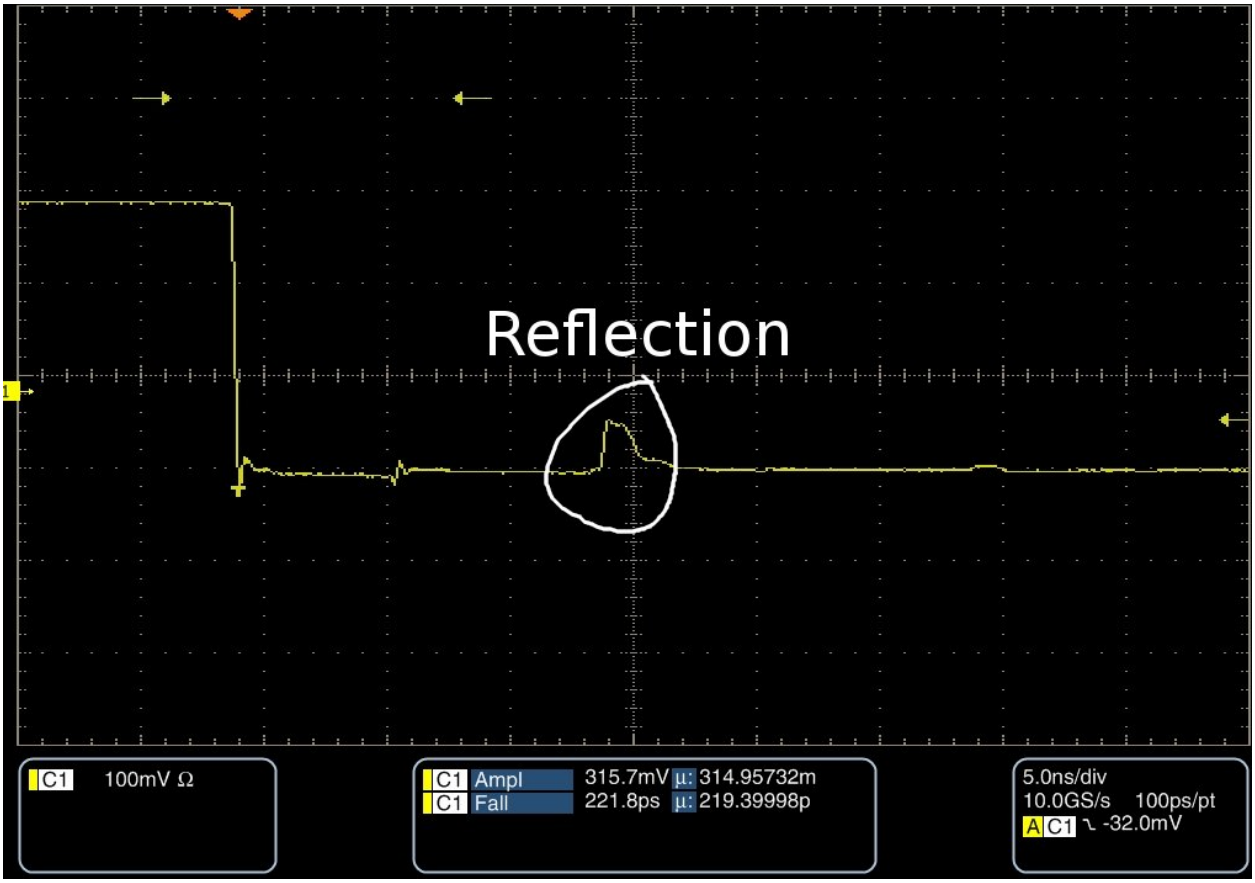

Figure 7: A fast pulse (with rise time < 90 ps) fed into one channel of the 25 μm MCP-PMT TL #5 and the resulting reflection, revealing an impedance mismatch. Similar results were obtained for the 10 μm TL-MCP-PMT while no reflections were seen for the bare TL readout board.